

Short Communication

Enhanced Lithium Storage Properties of Hierarchical MoS₂-rGO Nanosheets

Yuan Yuan¹, Feifan Huang², Anqing Pan^{1,*}, Wei Xiao^{2,*}

¹ School of Materials Science and Engineering, Central South University, Changsha 410083, PR China. Fax: +86 0731 8876692; Tel: +86 0731 88836069;

² School of Resource and Environmental Sciences, Wuhan University, Wuhan 430072, PR China. Fax: +86 27 68775799; Tel: +86 27 68775799;

*E-mail: pananqiang@csu.edu.cn, gabrielxiao@whu.edu.cn

Received: 4 March 2017 / Accepted: 23 April 2017 / Published: 12 May 2017

Layered materials (e.g. MoS₂ and graphene oxides) with ordered two-dimensional channels for mass transfer are promising building blocks for energy storage devices. Herein, hierarchical MoS₂-reduced graphene oxide nanosheets (notated as MoS₂-rGO nanosheets) are produced by growing hierarchical MoS₂ nanosheets on GO sheets through an L-Cysteine-assisted hydrothermal process together with a subsequent thermal annealing treatment. When evaluated as an anode material for lithium-ion batteries, the hierarchical MoS₂-rGO nanosheets manifest high specific capacity (~1000 mA h g⁻¹ at 100 mA g⁻¹), enhanced cycling stability and good rate capability. The present GO provides a robust and highly conductive matrix for in-situ growth of ultrathin MoS₂ nanosheets. The hence enhanced electrical conductivity, shorter mass transfer paths and structural integrity/robustness facilitates the enhanced lithium storage capability of the hybrids. The present work highlights the merit of hybrid two-dimensional materials for energy storage.

Keywords: hierarchical nanostructures; nanosheets; MoS₂; grapheme; lithium-ion batteries

1. INTRODUCTION

Lithium-ion batteries (LIBs) are currently the predominant power source for portable electronics and have shown great promise in electric vehicles and smart grids, because of their advantages of high energy density, long lifespan, no memory effect, and environmental benignity [1-4]. Molybdenum disulfide (MoS₂) based electrode materials are regarded as promising anode materials for LIBs because of the high specific capacity [5, 6]. However, due to the high surface energy and interlayer van der Waals attraction, 2D nanostructures of MoS₂ are vulnerable to restacking and condensation during charge/discharge processes, which might result in reduced accessibility of

electrolyte and fast capacity fading [7, 8]. In addition, MoS₂ is a typical semiconductor, the resulting high ohmic polarizations of intrinsic MoS₂ electrodes inevitably deteriorate their electrochemical performance in high-rate applications [9, 10].

To curb the above embarrassments, incorporation of MoS₂ into conducting scaffolds is promising. Conducting matrix in the corresponding hybrids could enhance electron transport [11]. Among different of conducting matrix, graphene oxides (GO) and the derived reduced GO (rGO) and graphene are intriguing in terms of excellent electrical conductivity, thermal/chemical stability, structural robustness and two-dimensional microstructures with ample surface chemistry [12-15]. Because of the extraordinary electrical conductivity of GO, growing MoS₂ on the surface of the as-prepared GO could enhance its electrochemical performance [16, 17]. There are several attempts on making MoS₂/GO composites among which Chen and coworkers are the pioneers [11]. For they have reported the work of in situ growing MoS₂ on GO, with the specific capacity and enhanced rate capability as the 2D nanoflake structure. What's more, the MoS₂/GO composites also showed the excellent performance for Sodium-Ion Batteries due to the structural robustness and two-dimensional microstructures with ample surface chemistry [18, 19].

In the present manuscript, hierarchical MoS₂-reduced graphene oxide (MoS₂-rGO) nanosheets by growing hierarchical MoS₂ nanosheets on GO sheets are produced through a facile hydrothermal treatment. There are many functional groups on the surface of GO, such as hydroxyl groups, therefore, MoO₄²⁻ adsorbing onto the GO tightly, which results in the formation of hierarchical MoS₂-rGO nanocomposites. Dissimilar from the previous reports on the formation of face-to-face MoS₂/G composites, the present MoS₂ nanosheets are perpendicularly aligned on rGO. As-prepared hierarchical MoS₂-rGO nanosheets show better reversible cycling performance and more excellent rate capability than the layer-by-layer hybrids of MoS₂ and reduced graphene synthesized by Jing which may be attributed to the distinct structure described above [20]. This unique packing manner between the two two-dimensional components tends to facilitate formation of hybrid with higher MoS₂ loading, more uniform mixing and more robust hierarchical structure. When evaluated as an anode material for LIBs, the hierarchical MoS₂-rGO nanosheets manifest high specific capacity, enhanced cycling stability and good rate capability

2. EXPERIMENTAL SECTION

First of all, the GO made by hummers method requires ultrasonication to make it evenly mixed with the solution, Then transfer 30mg GO into 40 ml deionized water, which followed by ultrasonication for about an hour [21, 22]. Then, 0.6 g of sodium molybdate (Na₂MoO₄·2H₂O) and 2.5 g of L-cysteine were weighed into the obtained homogeneous solution, after stirring and ultrasonication for another half an hour, followed by the step of the tightly sealed autoclave which filled with as-prepared solution was transferred into oven at 220 °C for the whole day. Waiting for cooling naturally, the black precipitates were taken out and the next step was washing them several times with water and ethanol, and then dried in an oven. The resulting black powder was then annealed at 800 °C for 2 hours in a 5% H₂/95%N₂ atmosphere. The preparation of the bare MoS₂ prepared as a comparison.

Both MoS₂-rGO and MoS₂ are characterized on the X-ray diffraction (Bruker D8 Advanced X-Ray Diffractometer with Cu K α radiation, $\lambda = 1.5406 \text{ \AA}$). Field-emission scanning electron microscope (FESEM) and Transmission electron microscope (TEM) images were obtained using a JEOL JSM-6700F microscope and a JEOL JEM-2100F microscope, respectively.

The electrochemical tests were totally performed with two-electrode Swagelok-type cells. By coating the slurry of the MoS₂-rGO mixture, conductive carbon black (Super-P-Li), and poly(vinylidene fluoride) (PVDF) binder (70:20:10 wt%) dissolved in N-methyl-2-pyrrolidinone (NMP) onto the copper foil, the electrode was completed. The electrolyte was a 1M LiPF₆ of the integration into the ethylene carbonate (EC) and diethyl carbonate (DEC) in the mass ratio of 1:1. The cells were assembled by using an Ar-filled glovebox and using the lithium metal foil for the counter electrode. The performance of the charge–discharge was in the voltage of 0.05 to 3.0 V.

3. RESULTS AND DISCUSSION

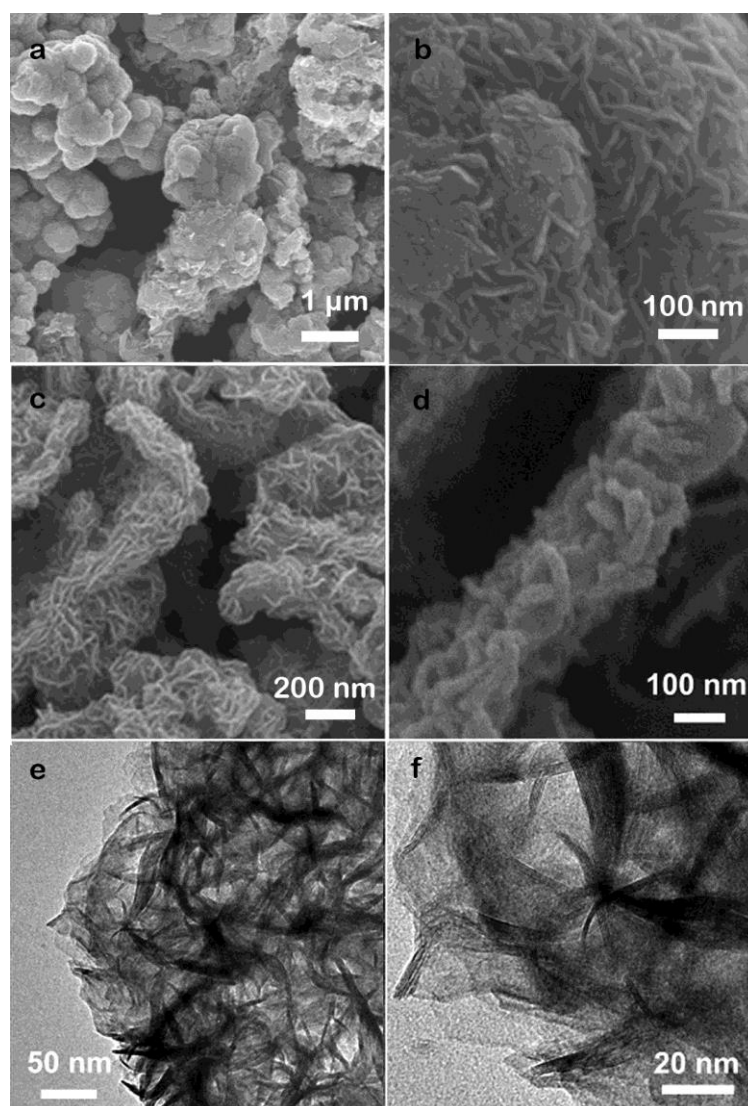


Figure 1. FESEM and TEM images of the prepared individual MoS₂ and the hierarchical MoS₂-rGO nanosheets.

Figs. 1a and 1b show the FESEM images of the obtained individual MoS₂. It is observed that the obtained MoS₂ consists of highly aggregated nanoflakes tends to assemble into large-size aggregations (microspheres herein) to minimize the surface energies. Fig. 1c and 1d show the FESEM images of the prepared hybrid. It is clearly shown that hierarchical two-dimensional architectures are predominant, ultrathin MoS₂ nanosheets (less than 5 nm) are perpendicularly grown onto GO sheets with large lateral sizes. By comparing the microstructure of individual MoS₂ (Figs. 1a and 1b) and MoS₂-rGO (Figs. 1c and 1d), the present GO plays a vital role on the formation of the hierarchical two-dimensional nanostructures. Firstly, GO could function as structure directing agents to curb ultrathin MoS₂ nanosheets from aggregation and overgrowth. Moreover, GO sheets provide spacious sites for nucleation and growth of MoS₂ nanosheets, facilitating high MoS₂ loading in the hybrid and porous structure among the nanosheets. Fig. 1e and 1f show the TEM images of the prepared hybrid. The nanoporous structure among MoS₂ nanosheets is clearly shown in the TEM images, which is beneficial to mass transfer upon electrochemical reactions.

The crystallographic phase and phase purity of the prepared individual MoS₂ and hierarchical MoS₂-rGO nanosheets are examined by X-ray powder diffraction (XRD). As shown in Fig. 2, the both XRD patterns can be well indexed to hexagonal MoS₂ (JCPDS card no. 37-1492; space group: *P6₃/mmc*, *a* = 3.161 Å, *c* = 12.299 Å). The characteristic (002) peak at 12° assigned to rGO is found absent in the pattern for the hybrid. In the hybrid, the content of rGO is relatively low. More important, the rGO sheets are homogeneously dispersed and coated with MoS₂ nanosheets [19, 23]. Any diffraction peaks from residues or impurities are also absent on the both patterns, indicating the high purity of the product [24-27].

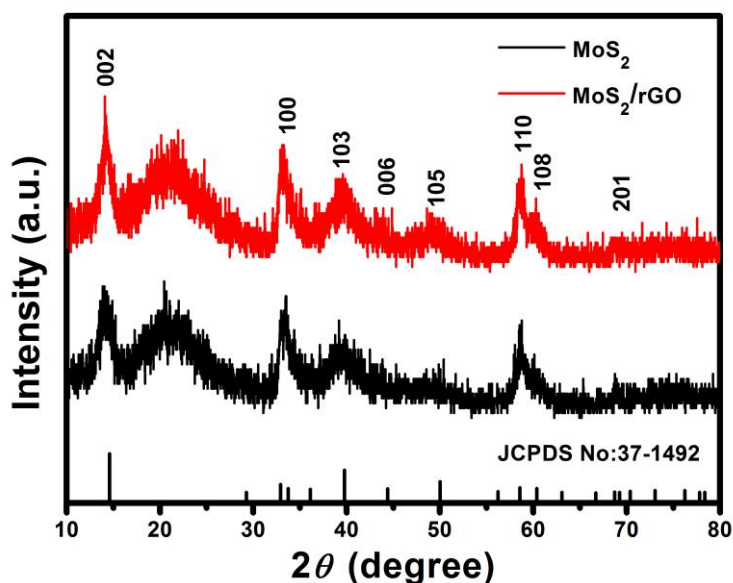


Figure 2. XRD patterns of the hierarchical MoS₂-rGO nanosheets and the prepared individual MoS₂.

Fig. 3a shows the representative discharge-charge voltage curves of the hierarchical MoS_2 -rGO nanosheets at a current density of 100 mA g^{-1} . Two plateaus at around 1.2 and 0.7 V are observed in the first discharge process. The plateau at 1.2 V is attributed to the formation of Li_xMoS_2 , and the lower plateau at 0.6 V corresponds to the decomposition of Li_xMoS_2 into Mo nanoparticles embedded into a Li_2S matrix. In the second and third discharge sweeps, the hierarchical MoS_2 -rGO nanosheets electrode shows two potential plateaus at 1.9 and 1.1 V. One plateau at about 2.2 V is observed for the charge processes, and this plateau is related to the extraction of Li^+ ion from the Li_2S matrix [24, 28-31].

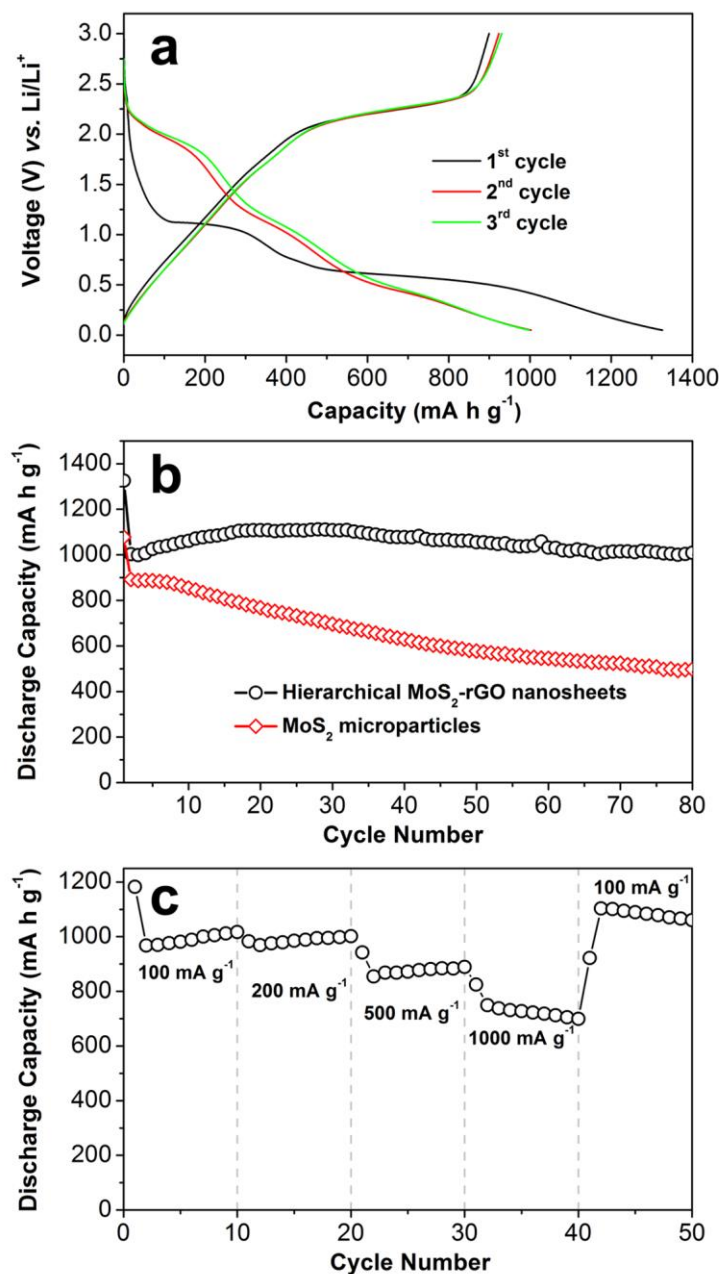


Figure 3. (a) Discharge-charge voltage profiles of hierarchical MoS_2 -rGO nanosheets. (b) Cycling performance of hierarchical MoS_2 -rGO nanosheets and MoS_2 microparticles within a voltage range of 0.05–3.0 V vs Li/Li^+ at a current density of 100 mA g^{-1} . (c) Rate capability of hierarchical MoS_2 -rGO nanosheets between 0.05 and 3.0 V.

The discharge-charge cycling performance is evaluated at a current density of 100 mA g⁻¹ for 80 cycles in Fig. 3b. As expected, these hierarchical MoS₂-rGO nanosheets manifest high specific capacity of 1010 mA h g⁻¹ and excellent cycling stability with almost no fading of capacity over the first 80 cycles. For comparison, the cycling performance of MoS₂ nanosheet aggregated micro-particles (Fig. 1a and 1b) exhibit much faster capacity fading. The hierarchical MoS₂-rGO nanosheets also exhibit greatly improved cycling response to a continuously varying current density. While cycling at high rates of 100–1000 mA g⁻¹, capacities of 700–1100 mA h g⁻¹ can still be retained, as shown in Fig. 3c. Evidently, these hierarchical MoS₂-rGO nanosheets demonstrate much enhanced lithium storage performance.

4. CONCLUSIONS

In summary, hierarchical two-dimensional micro/nano structure consisting of ultrathin MoS₂ nanosheets directly and vertically grown on rGO sheets was constructed and rationalized. When evaluated as an anode material for LIBs, the hierarchical MoS₂-rGO nanosheets demonstrates high reversible capacities of 1010 mAh g⁻¹ over 80 cycles at current densities of 100 mA g⁻¹, and remarkable capacity retention at increased current densities. This synthesis strategy demonstrated here could be extended to other nanostructured electrode materials and provides efficient routes for mass production of advanced electrode materials for LIBs.

ACKNOWLEDGEMENTS

This work was funded by the Fund for Fostering Talents in Basic Science of the National Natural Science Foundation of China (J1103409), National Natural Science Foundation of China (No. 51302323), Program for New Century Excellent Talents in University (NCET-13-0594).

References

1. Y. Sun, S. Gao, Y. Xie, *Chem. Soc. Rev.*, 43 (2014) 546
2. H. Hwang, H. Kim, J. Cho, *Nano Lett.*, 11 (2011) 4830.
3. Y. Zhang, A. Pan, L. Ding, Z. Zhou, Y. Wang, S. Niu, S. Liang, G. Cao, *ACS Appl Mater Interfaces*, 9 (2017) 3633.
4. S. Liang, X. Cao, Y. Wang, Y. Hu, A. Pan, G. Cao, *Nano Energy*, 22 (2016) 58.
5. L.C. Yang, S.N. Wang, J.J. Mao, J.W. Deng, Q.S. Gao, Y. Tang, O.G. Schmidt, *Adv. Mater.*, 25 (2013) 1184.
6. S. Ding, J.S. Chen, X.W. Lou, *Chem. Eur. J.*, 17 (2011) 13145.
7. Y. Chen, B. Song, X. Tang, L. Lu, J. Xue, *Small*, 10 (2014) 1543.
8. P. Wang, H. Sun, Y. Ji, W. Li, X. Wang, *Adv. Mater.*, 26 (2014) 969.
9. S. Tongay, J. Zhou, C. Ataca, K. Lo, T.S. Matthews, J. Li, J.C. Grossman, J. Wu, *Nano Lett.*, 12 (2012) 5580.
10. A. Castellanos-Gomez, M. Barkelid, A.M. Goossens, V.E. Calado, H.S. van der Zant, G.A. Steele, *Nano Lett.*, 12 (2012) 3192.
11. K. Chang, W. Chen, *Chem. Commun.*, 47 (2011) 4254.
12. Y. Zhang, A. Pan, S. Liang, T. Chen, Y. Tang, X. Tan, *Materials Letters*, 137 (2014) 177.

13. Z. Luo, J. Zhou, L. Wang, G. Fang, A. Pan, S. Liang, *J. Mater. Chem. A*, 4 (2016) 15308.
14. Y. Liu, Y. Wang, Y. Zhang, S. Liang, A. Pan, *Nanoscale Res. Lett.*, 11 (2016) 549.
15. X. Zhou, L.J. Wan, Y.G. Guo, *Chem. Commun.*, 49 (2013) 1840.
16. R. Li, *Int. J. Electrochem. Sci.*, (2017) 154.
17. Y. Liu, *Int. J. Electrochem. Sci.*, (2017) 2519.
18. L. Zhang, X.W. Lou, *Chem. Eur. J.*, 20 (2014) 5223.
19. S. Yang, X. Feng, S. Ivanovici, K. Mullen, *Angew Chem.*, 49 (2010) 8411.
20. Y. Jing, E.O. Ortiz-Quiles, C.R. Cabrera, Z. Chen, Z. Zhou, *Electrochimica Acta*, 147 (2014) 400.
21. W.S. Hummers, R.E. Offeman, *J. Am. Chem. Soc.*, 80 (1958) 1339.
22. Y.Y. Liang, H.L. Wang, H.S. Casalongue, Z. Chen, H.J. Dai, *Nano Res.*, 3 (2010) 705.
23. K. Bindumadhavan, S.K. Srivastava, S. Mahanty, *Chem. Commun.*, 49 (2013) 1825.
24. X. Cao, Y. Shi, W. Shi, X. Rui, Q. Yan, J. Kong, H. Zhang, *Small*, 9 (2013) 3438.
25. Y. Gong, S. Yang, Z. Liu, L. Ma, R. Vajtai, P.M. Ajayan, *Adv. Mater.*, 25 (2013) 3979-3984.
26. S.K. Park, S.H. Yu, S. Woo, B. Quan, D.C. Lee, M.K. Kim, Y.E. Sung, Y. Piao, *Dalton Trans.*, 42 (2013) 2405.
27. J.Z. Wang, L. Lu, M. Lotya, J.N. Coleman, S.L. Chou, H.K. Liu, A.I. Minett, J. Chen, *Adv. Energy Mater.*, 3 (2013) 805.
28. K. Chang, W. Chen, *ACS Nano*, 5 (2011) 4728.
29. T. Stephenson, Z. Li, B. Olsen, D. Mitlin, *Energy Environ. Sci.*, 7 (2014) 231.
30. X. Zhou, L.J. Wan, Y.G. Guo, *Nanoscale*, 4 (2012) 5871.
31. X. Huang, Z. Zeng, H. Zhang, *Chem. Soc. Rev.*, 42 (2013) 1946.

© 2017 The Authors. Published by ESG (www.electrochemsci.org). This article is an open access article distributed under the terms and conditions of the Creative Commons Attribution license (<http://creativecommons.org/licenses/by/4.0/>).